Energetics of vicinal Si(111) steps using empirical potentials

S. Kodiyalam, K.E. Khor, N.C. Bartelt, E.D. Williams, and S. Das Sarma
Department of Physics, University of Maryland, College Park, Maryland 20742-4111
(Received 17 June 1994; revised manuscript received 17 November 1994)

Motivated by recent experimental determinations of step energies on the high-temperature 1×1 reconstructed phase of Si(111), we have calculated step and step-step interaction energies using empirical potentials. Two distinct configurations of atoms along the step edge are plausible: configurations with atoms on the upper terrace that could rebond with atoms on the lower terrace and others without these atoms. By considering two different empirical potentials, only one of which allows this rebonding, we show that the rebonding gives rise to a behavior inconsistent with experiments probing step-step interactions. For configurations without the rebonding the step-step interaction coefficient is in the range 0.00–0.39 eV Å, roughly agreeing with the experimental estimate of approximately 0.15 eV Å. With the rebonding, however, the step-step interaction coefficient for the $[\bar{1}\,\bar{1}2]$ steps is 4.5 eV Å, much larger than the experimental estimate. This suggests that rebonding does not occur. Kink energies are also calculated from the orientational dependence of the step energies and compared with experiment. These calculations show that kink-kink interactions are negligible although there are significant corner energies.

I. INTRODUCTION

There is a growing body of experimental work involving step dynamics on semiconductor[1,2] and metal surfaces.[3–5] These experiments measure step fluctuations, specifically the time dependence of terrace width distributions, to obtain information about step energetics. Theoretical models to explain these observations have been based on the Langevin formalism.[2,6] This formalism, however, does not directly allow the atomic processes by which the steps fluctuate to be obtained. The equilibrium properties of steps on Si(111) have recently been described using a simple terrace-step-kink model to fit experimental data on the orientational phase diagram of vicinal surfaces.[7] The work here is motivated by the need for theoretical estimates of the microscopic parameters such as the step, kink, and step-step interaction energies that are used in such models.

We will focus on interpreting recent experiments which have determined step energies on 1×1 reconstructed Si(111) using observations of step fluctuations, step distributions,[1,2,7] and observations of sublimation holes.[8] The step-step interactions on this surface have also been estimated.[1,7] Observations of circular step systems at high temperature[1,9] suggest that the step free energy is isotropic. Our work here is aimed at verifying if the zero-temperature energetics are consistent with these high-temperature observations, particularly with regard to anisotropy in step energy, by directly calculating them using the empirical potentials of Stillinger-Weber and Khor–Das Sarma. Specifically, kink energies calculated here may be compared to those used previously in statistical mechanical fits to experimental data.[7] As there is no direct evidence that the observed step-step interactions are due to elastic relaxations, these interactions are calculated here to see if the elastic hypothesis is indeed plausible.

We find in this study that these two potentials predict significantly different energetics for steps on Si(111), both differing from the fit of a square lattice model to experiment.[7] However, there are robust trends, i.e., common features predicted by both the potentials. Differences between the predictions of the two potentials, the common trends and disagreements with experiment, are interpreted in the discussion and conclusion sections of the paper.

II. POTENTIALS

Understanding step energetics on Si(111) requires an understanding of the rebonding that occurs at the step edges which reduce the dangling bonds. This rebonding is similar in nature to the rebonding that occurs in the dimer reconstruction on Si(100). The Stillinger-Weber potential[10] gives reasonable results for this reconstruction on Si(100),[11] and for properties of steps on Si(100).[12,13] The use of a second empirical potential in this study is mainly motivated by the need to identify the results that are independent of the details of the potential. It must, however, be noted that the Stillinger-Weber potential does not give any reconstruction of the Si(111) surface and the predicted adatom energetics on this surface are not satisfactory.[14] Similarly, although the Khor–Das Sarma potential reproduces bulk properties[15] and the dimerization on Si(100), it needs additional modification to predict adatom energetics on Si(111) correctly. Reproduction of the dimer reconstruction on Si(100) by both potentials [and properties of steps on Si(100) by the Stillinger-Weber potential] is however an encouraging feature as most of the configurations in our study have step-kink facets that are locally (100). Further, the Khor–Das Sarma potential has parameters which are tuned to handle cases when the coordination number is not equal to four, specifically π bonding in graphitelike configurations that occur on the Si(111) surface. The predictions of the two potentials can therefore be regarded as rough estimates of the step-kink energetics.

A. Stillinger-Weber (SW)

This potential[10] consists of two- and three-body terms of the following form:

$$V = \sum_{i<j} V_2(\vec{r}_i, \vec{r}_j) + \sum_{i\neq j\neq k\neq i} V_3(\vec{r}_i, \vec{r}_j, \vec{r}_k) \ , \tag{1}$$

where

$$V_2(\vec{r}_i, \vec{r}_j) = \begin{cases} A\epsilon \left[B\left(\frac{r_{ij}}{\sigma}\right)^{-p} - \left(\frac{r_{ij}}{\sigma}\right)^{-q}\right] e^{\left(\frac{r}{\sigma} - a\right)^{-1}} & , \ r_{ij} < a\sigma \\ 0 & , \ r_{ij} \geq a\sigma \end{cases} \tag{1a}$$

and

$$V_3(\vec{r}_i; \vec{r}_j, \vec{r}_k) = \begin{cases} \lambda\epsilon \left(\cos\theta_{jik} + \frac{1}{3}\right)^2 \exp\gamma \left[\left(\frac{r_{ij}}{\sigma} - a\right)^{-1} + \left(\frac{r_{ik}}{\sigma} - a\right)^{-1}\right] & , \ r_{ij} \text{ and } r_{ik} < a\sigma \\ 0 & , \ r_{ij} \text{ and/or } r_{ik} \geq a\sigma \end{cases} \tag{1b}$$

with

$$r_{ij} = \mid \vec{r}_i - \vec{r}_j \mid \ , \ \theta_{jik} = \cos^{-1}\left[\frac{(\vec{r}_i - \vec{r}_j)\cdot(\vec{r}_i - \vec{r}_k)}{r_{ij}r_{ik}}\right] . \tag{1c}$$

The parameters of this potential are chosen to make the diamond structure the most stable and also give a liquid structure (the pair correlation function) which is in reasonable accord with experiment. The length scale σ and the energy scale ϵ are chosen to give the observed lattice spacing and cohesive energy of crystalline silicon at zero temperature. The parameter values are listed in Table I.

B. Khor–Das Sarma (KD)

This is a many-body potential[15] consisting of pairwise interactions moderated by the local environment:

$$V = \frac{1}{2}\sum_i \sum_{j\neq i} V_{ij} \ , \tag{2}$$

where

$$V_{ij} = AZ_{ij}\left\{e^{-\theta r_{ij}} - \frac{B_o}{Z^{\alpha}_{i\,\text{eff}}} e^{-\lambda r_{ij}} \times \left[1 + \sum_{k\neq i,j} \{\cos[\eta(\theta_{jik} - \theta_i)] - 1\} Z_{ij}\right]\right\} \tag{2a}$$

TABLE I. Parameters of the potentials used in the simulations.

Potential parameters		
	SW potential	
A=7.049556277	B=0.6022245584	p=4
$q = 0$	$a = 1.8$	λ=21
γ=1.2	ϵ =1 (2.168256721 eV)	σ = 1(2.0951 Å)
	KD potential	
A = 2794.2386 (eV)	B_0=0.08251716	θ = 3.13269 (Å^{-1})
λ = 1.34146 (Å^{-1})	α = 0.6249096	γ =3.38218
β =25.44123 (Å$^{-\gamma}$)	η =0.90084597	f = 25 (Å^{-1})
$C_0 = 3.8$	$C_1 = \frac{0.1}{9}$	$C_2 = -\frac{2.35}{9}$
$C_3 = \frac{2.6}{9}$	$C_4 = \frac{1.45}{9}$	
$D_0 = 2.358083636$	$D_1 = 0.07598029648$	
$D_2 = -0.2876355442$	$D_3 = 0$	
	Modified KD potential	
$C_0 = 3.8$	C_1=−0.3	$C_2 = 0.2$
$C_3 = 0.3$	$C_4 = 0$	
$D_0 = -3.844080610$	$D_1 = 13.65684306$	
$D_2 = -10.00769657$	$D_3 = 2.272812689$	

with

$$r_{ij} = |\vec{r_i} - \vec{r_j}|, R_i = \left(\sum_{j\neq i} \frac{e^{-fr_{ij}}}{r_{ij}}\right)^{-1} \rightarrow \begin{matrix}\text{minimum } (r_{ij}) \\ j \neq i\end{matrix}, \tag{2b}$$

$$Z_{ij} = e^{\beta(r_{ij} - R_i)^\gamma}, \quad \theta_{jik} = \cos^{-1}\left[\frac{(\vec{r_i} - \vec{r_j}) \cdot (\vec{r_i} - \vec{r_k})}{r_{ij} r_{ik}}\right], \tag{2c}$$

$$Z_{i\,\text{eff}} = C_0 + C_1(Z_i - 3) + C_2(Z_i - 3)^2 + C_3(Z_i - 3)^3 + C_4(Z_i - 3)^4,$$
$$\theta_i = D_0 + D_1(\ln Z_i) + D_3(\ln Z_i)^2 + D_4(\ln Z_i)^3, \tag{2d}$$

where

$$Z_i = \sum_{j\neq i} Z_{ij} \tag{2e}$$

is a measure of the number of nearest neighbors. Further, V_{ij} is explicitly cutoff, i.e., $V_{ij} = 0$ if $r_{ij} \geq 3.8$ Å. The parameters of the potential (with $Z_{i\,\text{eff}} = Z_i$ and $\eta = 0$) are chosen to reproduce the linear variation of $\ln(Z)$ and $\ln(-V_{\text{equil}}$ per atom$/Z)$ (all $Z_i = Z$) with equilibrium interatomic distance for a wide range of structures of silicon, as well as the bulk modulus of the diamond structure. The polynomial in $\ln(Z_i)$ for θ_i is chosen such that the original results for the graphitic, diamond, and simple cubic structures are recovered: $\theta_i = \cos^{-1}(-1/2)$, $\cos^{-1}(-1/3)$, and $\cos^{-1}(0)$ for $Z = 3$, 4, and 6, respectively. The parameter η is then fitted [with $Z_{i\,\text{eff}} = Z$ and $\theta_i = \cos^{-1}(-1/3)$] to obtain the bond bending force constant of the diamond structure.

In this study, the polynomial in Z_i for $Z_{i\,\text{eff}}$ is chosen such that the gradient of the potential is continuous across $Z_i = 4$: Since $Z_{i\,\text{eff}} = Z_i$ for $Z_i \geq 4$, $dZ_{i\,\text{eff}}/dZ_i = 1$ at $Z_i = 4$. Further, $Z_{i\,\text{eff}}(Z_i = 3) = 3.8$ so that the bond strength agrees to scaled results in carbon chemistry for the sp^2-sp^3 bond.[16] Additional fitting such that $Z_{i\,\text{eff}}(Z_i = 2) = 3.4$ and $Z_{i\,\text{eff}}(Z_i = 1) = 3.0$ has been done somewhat arbitrarily: the only requirement being that $Z_{i\,\text{eff}}$ not become small for $Z_i \approx 1$ ($Z_{i\,\text{eff}} = 3.4$ corresponds to the bond strength of an sp-sp^3 bond[16]).

In the simulations with the Khor–Das Sarma potential, the above-mentioned functional forms for $Z_{i\,\text{eff}}$ and θ_i were used. However, the results showed that in some of the step-kink configurations [Figs. 3(f) and 3(i)] there were some atoms with $Z_i \approx 2$. As no particular fitting was done in this range of Z_i either for $Z_{i\,\text{eff}}$ or θ_i, there is no reason for the energetics to be correct in such configurations. Thus for the configuration with the largest number of such atoms per unit length of step, Fig. 3(c), the energetics have been recalculated using a different fit based on the following argument: In such configurations the atom with $Z_i \approx 2$ is bonded to an atom with $Z_i \approx 3$ and another with $Z_i \approx 4$. Hence, assuming that (i) the bonding is through two p orbitals so that the bond angle is 90° and that the bond strength with the $Z_i \approx 4$ atom is that of a p-sp^3 bond, and further assuming that (ii) the bond strength with the $Z_i \approx 3$ atom is the sum of a p-sp^3 and a π bond, (iii) the p-sp^3 bond strength is the average of p-p and sp^3-sp^3 bond strengths, and (iv) the p-p bond strength $\approx 1/6$ the energy per atom in the simple cubic structure, then it can be seen using the data in Refs. 15 and 16 that the average bond strength of the atom with $Z_i \approx 2$ is very close to the sp^3-sp^3 or the diamond structure bond strength. Therefore the modified KD potential has $Z_{i\,\text{eff}}(Z_i = 2) = 4$ and $\theta_i(Z_i = 2) = 90°$. The parameters of the potential with the two fits for $Z_{i\,\text{eff}}$ and θ_i are shown in Table I.

III. STRUCTURAL ENERGIES

A. Molecular-dynamics method

The molecular-dynamics cell, sketched in Fig. 1, is configured such that it allows for at most one single height step with at most one unit depth kink. It consists of

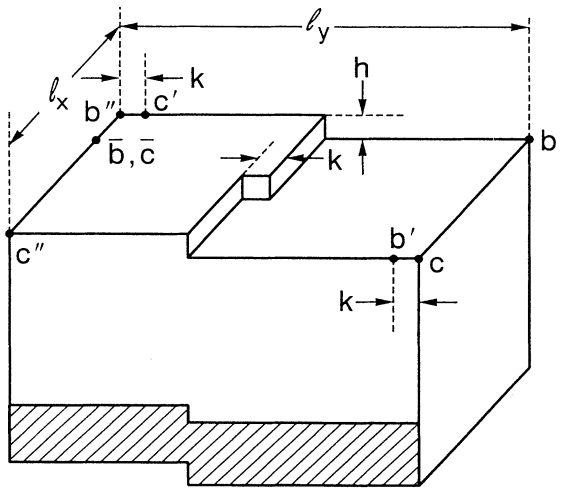

FIG. 1. The molecular-dynamics cell, used in the calculations. The shaded region consists of three Si(111) bilayers with atoms fixed at diamond lattice coordinates. Periodic boundary conditions applied along the x axis by the association of points $b - b'$ and $c - c'$, and along the y axis by the association of points $b - b''$ (or $\bar{b}$) and $c - c'$ (or $\bar{c}$).

a chosen number of bilayers of Si(111) with the bottom three bilayers (shaded region) having atoms fixed at the diamond lattice coordinates throughout the simulation. The z axis is perpendicular to the bilayer and the x axis is along one of the two surface lattice constants, a_1 or a_2, as shown in Fig. 2. Periodic boundary conditions are applied along the x and y axis: the points $b-b'$ and $c-c'$ showing the association along the x axis, the points $b-b''$ and $c-c''$ showing the association along the y axis. When the $b-b''$ and $c-c''$ association is not possible (the x axis along the $[\bar{1}01]$ step), the association is shown by $b-\bar{b}$ and $c-\bar{c}$.

The system potential energy E is computed in such a way that only the moving atoms constitute the system. Hence, in addition to all the interactions between moving atoms, in case of the SW potential, only half of any two-body interaction between a fixed and a moving atom is included in E. The fraction of the three-body interaction included is equal to 1/3 if only one of the three atoms is moving, and 2/3 if two of the three atoms are moving. Similarly, for the KD potential, in addition to all interactions between moving atoms, only half of any pairwise interaction between a fixed and a moving atom is included in this energy.

For every configuration studied, the initial coordinates of the atoms near the step edge are changed from their corresponding bulk values so as to minimize the potential energy. The initial velocities are maxwellian distributed so that the system is at a small "temperature." With this initialization the potential energy of the system is minimized using the following cycle:

(a) Integration of Newtons law (with dissipation):

$$m\frac{d^2\vec{r_i}}{dt^2} = -\nabla_{\vec{r_i}}V \left\{-\gamma\frac{d\vec{r_i}}{dt}\right\} . \tag{3}$$

(b) Integration of the steepest-descent equations:

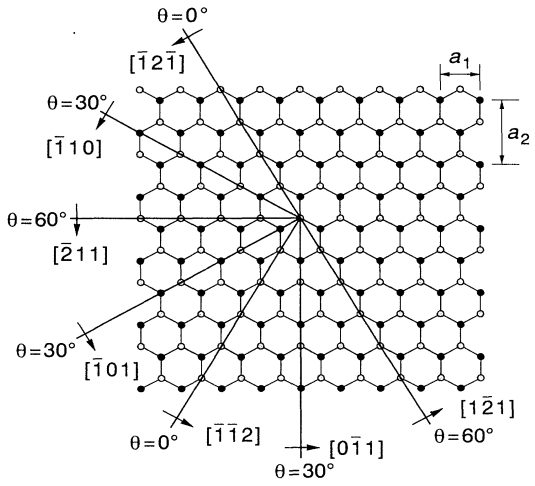

FIG. 2. One bilayer of the Si(111) surface consisting of the upper monolayer (gray) and the lower monolayer (black). The figure shows the threefold and reflection symmetry of this surface: Steps running along directions with equal θ have equal energy.

$$\frac{d\vec{r_i}}{ds} = -\nabla_{\vec{r_i}}V . \tag{4}$$

Typically, the above cycle is repeated five times. However, only in the first cycle is dissipation used to reduce the "temperature" (kinetic energy) of the system. The dissipation is not continuous so as to allow the system to reach "equilibrium" at each temperature. In subsequent cycles there is no dissipation and the system begins with zero kinetic energy. This technique was efficient in reducing the potential energy, as any increase in the kinetic energy had to correspond to a decrease in potential energy.

Integration of the above equations was done using a fifth-order Gear algorithm.[17] In simulations with the SW potential the units of mass, length, and energy are chosen to be the mass of the silicon atom m, the parameters of the potential σ and ϵ, respectively. In simulations with the KD potential the same are chosen to be m, 1 Å, and 1 eV, respectively. In these units, the time step dt, the s step ds, and the dissipation factor γ were chosen to be 0.005, 0.001, and 0.2, respectively. The initial temperature in simulations with the SW (KD) potential was 0.0015 (0.003). The typical total number of time and s steps to obtain the minimum value of the system potential energy E for any configuration was 40 000.

B. Notation and definition

The step energy β is defined as

$$\beta = (E - N\epsilon_b - \epsilon_s\ell_x\ell_y)/(\ell_x^2 + k^2)^{\frac{1}{2}} , \tag{5}$$

where E is the minimum potential energy of the system with N atoms, ϵ_b is the bulk energy per atom, ϵ_s is the surface energy per unit area, k is the depth of one kink, and ℓ_x and ℓ_y are the molecular-dynamics cell dimensions (see Fig. 1) along the x and y axes, respectively. The numerator is the excess energy relative to the unstepped surface and the denominator is the corresponding length along the step. Only unit kinks and single height steps are considered in this study. Therefore the kink depth k and the step height h are constants. For a step with no kinks k vanishes. The surface energy ϵ_s is defined when there is no step ($h = 0, k = 0$) as

$$\epsilon_s = (E - N\epsilon_b)/\ell_x\ell_y . \tag{6}$$

Assuming that classical elasticity theory applies,[18] and that steps interact only through elastic dipole-dipole interactions, the functional form for β in terms of the angle (ξ) between the step and the x axis of the molecular dynamics cell, and the terrace width (t) measured perpendicular to the step edge, is given by

$$\beta(\xi, t) = \beta^0(\xi) + A(\xi)/t^2 , \tag{7}$$

where $\xi = \tan^{-1}(k/\ell_x)$ and $t = \ell_y\cos(\xi)$. This equation defines the energy of an isolated step β^0 and the step-step interaction coefficient A. Further neglecting kink-kink interactions, the step energy per unit length along

the x axis of an isolated step $\beta_x^0 \left\{ \stackrel{\text{def}}{=} \beta^0(\xi)[\cos(\xi)]^{-1} \right\}$ as a function of the kink-kink separation ℓ_x can be written as

$$\beta_x^0(\ell_x) = \beta^0(\xi = 0) + \epsilon_k/\ell_x \ , \tag{8}$$

where $\beta^0(\xi{=}0)$ is the energy of an unkinked step and ϵ_k is the kink energy.

Any plane intersecting the (111) surface defines a step. The step orientation is defined to be the direction of the projection of the normal of this plane in the step down direction onto the (111) surface. Figure 2 shows the Si(111) surface (one bilayer) and some of the step orientations. The steps along the high symmetry directions with orientations $[\bar{1}\,\bar{1}2]$ and $[\bar{2}11]$ are further defined to be at $\theta = 0°$ and $\theta = 60°$, respectively. Since the (111) surface has threefold as well as reflection symmetry it suffices to study steps whose orientations span the above range. This symmetry implies that steps running along directions with equal θ have equal energy. In this study this equivalence has been used to label steps and/or kinks by their normals or by the normals of steps equivalent to them. The range of θ for kinks on the $[\bar{1}\,\bar{1}2]$ step is $0° < \theta \leq 30°$ and for kinks on the $[\bar{2}11]$ step is $60° > \theta \geq 30°$. Hence, $\theta = \xi$ when the x axis is along the $[\bar{1}\,\bar{1}2]$ step and $\theta = 60° - \xi$ for the x axis along the $[\bar{2}11]$ step. The intermediate low symmetry direction ($\theta = 30°$) $[\bar{1}01]$ step can also be described as the step with the highest kink density along either of the two high symmetry direction steps. When the x axis is along this step $\theta = 30°$ and $\xi = 0°$.

Stresses for the Si(111) surface are calculated to estimate their contribution to step-step interactions (see Appendix A). The surface stress tensor is defined as $\sigma_{ij} = \partial\epsilon_s/\partial u_{ij}$ where u_{ij} is the surface strain tensor. The threefold symmetry of the surface implies that this stress is isotropic, i.e., $\sigma_{ij} = \sigma\delta_{ij}$. Hence, it is calculated in this study using $\sigma = [E(A_0 + dA) - E(A_0 - dA)]/(2A_0 dA)$ where A_0 is the equilibrium surface area and $dA/A_0 = 10^{-6}$. This method is the numerical implementation of the definition of surface stress as originally given by Shuttleworth.[19] The area is changed by stretching or compressing the molecular-dynamics cell. Since the stress is isotropic this can be done by scaling the initial x and/or the y coordinates of all the atoms. Surface energies ϵ_s and surface stresses σ are shown in Table II. The number of (111) bilayers (of moving atoms) used was 27. These results may be compared to Vanderbilt's *ab initio* local-density approximation (LDA) calculations.[20] It must be noted that the SW potential does not result in changes from the bulk terminated surface and therefore the surface energy is given by bond counting itself. Also to the accuracy quoted the modified KD potential gives the same surface properties as the standard KD potential as shown in Table II.

TABLE II. Surface energy (ϵ_s) and surface stress (σ).

	Surface properties	
Potential	ϵ_s(meV/Å^2)	σ(meV/Å^2)
SW	$-\frac{\epsilon_b}{2a_1a_2} \approx 84.9$	0
KD	87.8	−81.0
Modified KD	87.8	−81.0
ab initio LDA	114	−39

C. Step and kink configurations

Step-kink configurations considered in this study are shown in Figs. 3(a)–3(j). The figures show the initial configuration of atoms near the step edge used for simulation with the SW potential. The configurations are of two types: type A, without any rebonding possible between upper and lower terrace atoms, and type B, with such a rebonding possible. Both these types were investigated with the SW potential. However, during the simulation with the KD potential, configurations 3(h) and 3(j) were not studied since the step energy of configuration 3(b) was much higher than that of 3(a), and the 3(c) and 3(d) configurations had almost equal step energies. These results were expected from the initial configurations which

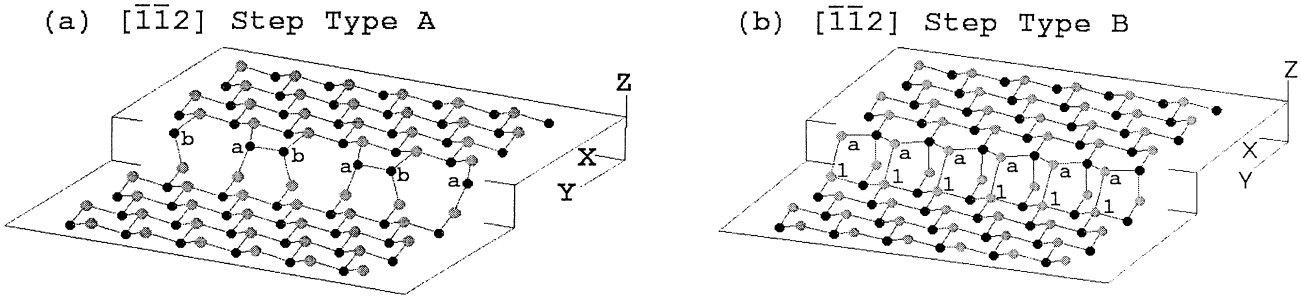

FIG. 3. (a) – (e) Initial step configurations. Atoms labeled by letters are displaced from bulk lattice coordinates. SW potential results in rebonding between all labeled atoms. KD potential results in rebonding only between atoms labeled by letters. Favorable configurations corresponding to the SW potential (type B) have step-step interactions an order of magnitude larger than experimental estimates. (f)–(j) Initial kink configurations. Atoms labeled by letters are displaced from bulk lattice coordinates. SW potential results in rebonding between all labeled atoms. KD potential results in rebonding only between atoms labeled by letters. Only the unfavorable configurations corresponding to the SW potential (type A_1) have the kink energy roughly consistent with experimental estimates.

showed that the rebonding was not favorable (when rebonding is forced the initial step energy increased). It was verified that forced rebonding in the initial 3(b) configuration nevertheless resulted in unbonded atoms in the final configuration. The [$\bar{2}11$] step of configuration type A is also considered as the "limiting configuration" corresponding to steps of configuration type B as the orientation approaches $\theta=60°$.

It should be noted that the magnitude of displacement (perpendicular and/or parallel to the step-kink edge) of atoms (near the step edge) from their corresponding bulk values in the initial configurations for the KD potential

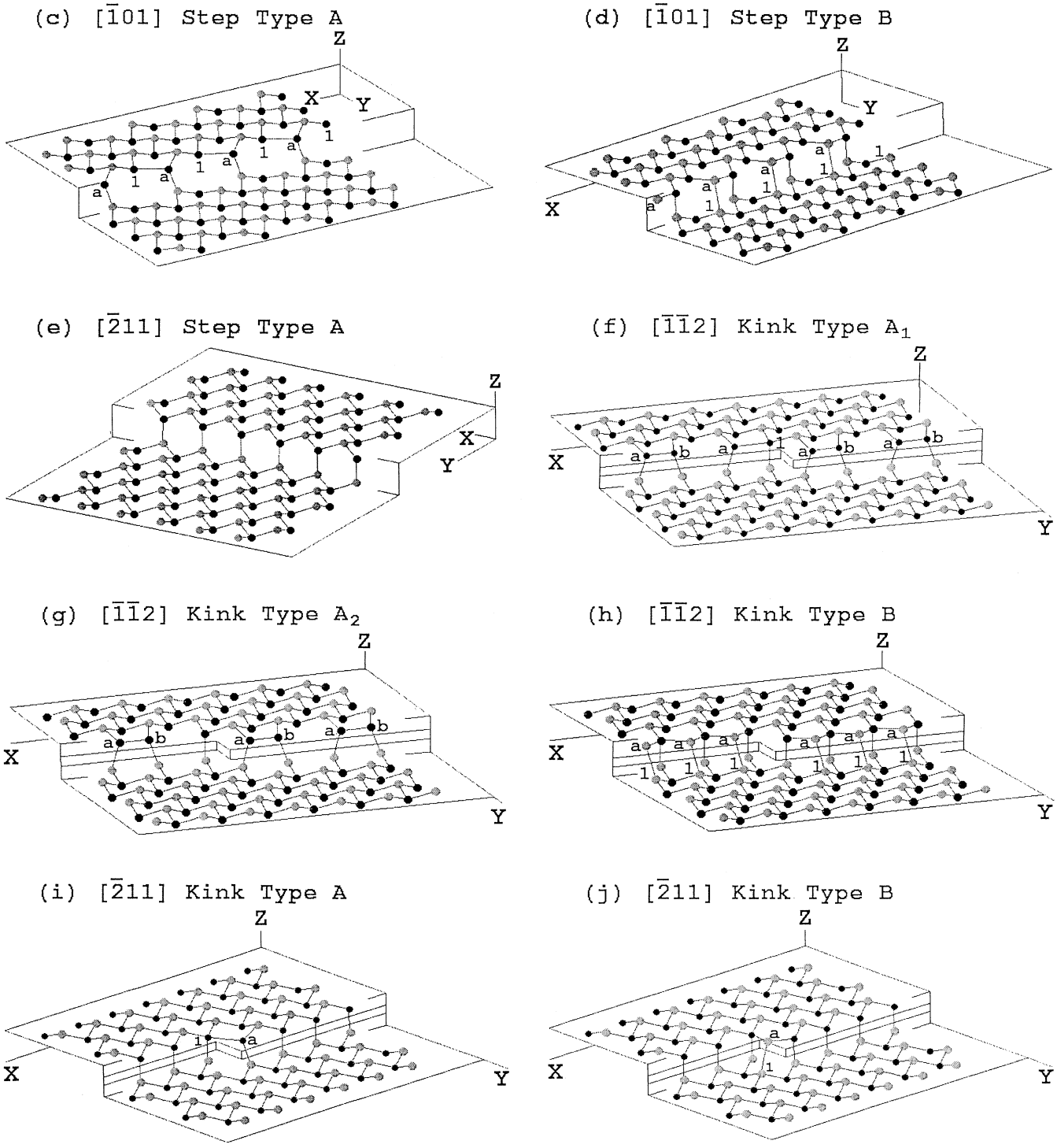

FIG. 3 *(Continued).*

may not be as shown in Fig. 3 (which corresponds to initial configurations investigated with the SW potential). All atoms labeled by letters are displaced from their corresponding bulk-terminated positions. However the initial displacement used with the KD potential was large (as shown) if it lowered the energy and very small if not. As a rule the SW potential favored significant displacement even if only one of the atoms (participating in rebonding parallel or perpendicular to the step-kink edge with the other atom) could be moved (i.e., had only two nearest neighbors before any displacement) whereas the KD potential favored this displacement only if both the rebonding atoms could be moved. For both potentials, rebonding between atoms in the final configuration was directly correlated to the displacements in the corresponding (low energy) initial configuration: Rebonding occurs if the displacement of an atom towards another was large and does not occur if it was very small.

The following are the system sizes along the x- and y-axes for periodic boundary conditions to apply:

$$\text{(111) surface: } \ell_x = n_1 a_1, l_y = n_2 a_2,$$

$$[\bar{1}\,\bar{1}2] \text{ step: } \ell_x = n_1 a_1, l_y = (n_2 - 2/3) a_2,$$

$$[\bar{1}\,\bar{1}2] \text{ kink: } \ell_x = (n_1 + 1/2) a_1, l_y = (n_2 - 2/3) a_2,$$

$$[\bar{1}01] \text{ step: } \ell_x = n_1 a_2, l_y = (n_2 - 2/3) a_1,$$

$$[\bar{2}11] \text{ kink: } \ell_x = (n_1 + 1/2) a_1, l_y = (n_2 - 1/3) a_2,$$

$$[\bar{2}11] \text{ step: } \ell_x = n_1 a_1, l_y = (n_2 - 1/3) a_2,$$

where a_1 and a_2 are surface lattice constants as shown in Fig. 2 and n_1 and n_2 are positive integers. Note that there are two types of $[\bar{1}\,\bar{1}2]$ kinks within configuration type A: A_1 when n_1 is odd and A_2 when n_1 is even. The system depth along the z axis is specified by n_3 which is the number of (111) bilayers (of moving atoms).

Since steps are defined by the intersection of a plane with the (111) surface, the configurations of the face also correspond to the surface of the intersecting plane [again the three fold and reflection symmetry about the (111) axis may be used to label surfaces by their normals or by the normals of the surfaces equal to them in energy]. Hence, surface energies can be calculated from the corresponding step energies. Specifically the (110) and (331) surfaces are the $[\bar{2}11]$ step configuration with n_2=1 and n_2=1.5, respectively. The (100), (311), and (211) surfaces are the $[\bar{1}\,\bar{1}2]$ step configuration with n_2=1, n_2=1.5, and n_2=2, respectively. The type (A or B) of the configuration determines the type of reconstruction on the corresponding surface.

D. Energetics

Table III shows the results of the simulation with the step configurations of Fig. 3. Isolated step energies β^0 and interaction coefficients A have been extracted by fitting the variation of the step energy with terrace width ℓ_y [configurations 3(a)–3(e) in Fig. 3] to Eq. (7) (with $\xi = 0$). Figure 4 is typical of the straight line fits attempted (when $n_3 = 27$). Success of this fitting procedure in all cases shows that the variation of step energy is consistent with elasticity theory in the chosen range(s) of terrace width(s) (n_2) as listed in Table III. It can be seen that a depth (n_3) of typically nine moving Si(111) bilayers is sufficient to obtain the step energies accurately. However, this is not the case with interaction coefficients as they probe very small variations in the step energy. Insufficient system depth results in slightly smaller interaction coefficients: a result that may not be evident

TABLE III. Energetics of unkinked step configurations: step energy (β^0) and step-step interaction strength (A). n_1 and n_2 are the system dimensions, in units of the appropriate surface lattice constant, along the x and y axes, respectively. n_3 is the depth of the system in number of (111) bilayers.

Unkinked step configurations											
		SW potential					KD potential				
Configuration	Type	System size			Energetics		Sytems size			Energetics	
		n_1	n_2	n_3	β^0 (meV/Å)	A (meV Å)	n_1	n_2	n_3	β^0 (meV/Å)	A (meV Å)
(I) $\bar{1}\,\bar{1}2$ step	A	2	5 to 11	9	162.2	$\to -0^+$	4	8 to 10	9	240.2	7.8×10^1
$\Rightarrow \theta = 0°$		2	5 to 14	27	162.2	$\to -0^+$	2	8 to 20	27	240.2	1.3×10^2
	B	2	2 to 10	9	39.0	4.5×10^3	2	8 to 10	9	347.8	1.9×10^2
		1	2 to 21	27	38.8	4.5×10^3	1	8 to 20	27	347.8	2.6×10^2
(II) $\bar{1}01$ step	A	1	6 to 18	10	188.4	2.4×10^2	1	8 to 10	9	323.8	1.1×10^2
$\Rightarrow \theta = 30°$		1	6 to 20	27	188.4	2.4×10^2	1	11 to 20	27	323.8	1.3×10^2
	B	1	5 to 15	10	152.6	1.5×10^3	1	8 to 10	9	322.0	1.5×10^2
		1	5 to 20	27	152.6	1.5×10^3	1	10 to 20	27	322.0	1.8×10^2
(III) $\bar{2}11$ step	A	4	4,7	12	$-\frac{\epsilon_b}{6a_1} \approx 188.2$	0.0	2	8 to 10	9	202.4	1.5×10^2
$\Rightarrow \theta = 60°$		1	1 to 14	27	$-\frac{\epsilon_b}{6a_1} \approx 188.2$	0.0	1	8 to 20	27	202.4	2.1×10^2
										Modified KD potential	
(I) $\bar{1}01$ step	A						1	11 to 20	27	361.5	3.9×10^2
$\Rightarrow \theta = 30°$											

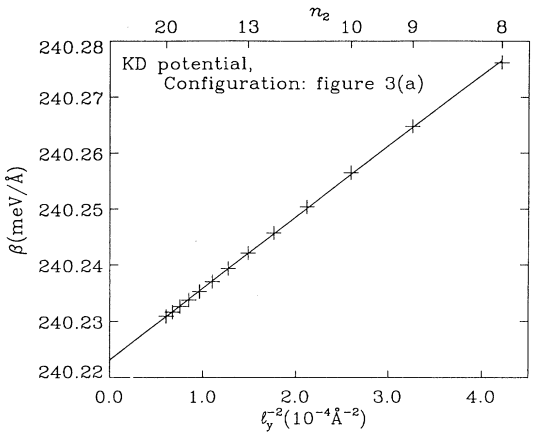

FIG. 4. Typical variation of the step energy β with the terrace width ℓ_y in a step configuration. The linear variation of β with ℓ_y^{-2} is consistent with elasticity theory. The intercept is the step energy β^0 and the slope is the step-step interaction coefficient A. The terrace width is linearly related to n_2.

from the table as the values are quoted to only two significant figures. The uncertainity in the calculated values for the interaction coefficients are due to the deviations from the expected ℓ_y^{-2} behavior. Step configurations with large interaction coefficients (>1 eV Å) and also some with small values (<0.4 eV Å) decrease as the terrace width (ℓ_y) increases. This decrease is at least in part due to insufficient system depth since it is observed to diminish as depth increases. The fitting to Eq. (7) in such cases has been done over the entire range of ℓ_y—larger ℓ_y naturally contributing less to the fit. Other step configurations with small values of interaction coefficient (< 0.4 eV Å) show a rise and saturate with increasing ℓ_y. In such cases the fitting to Eq. (7) has been done over the range of larger ℓ_y only. Table III also shows the result of simulation with the modified KD potential for the $[\bar{1}01]$ step (configuration type A). The step energy is relatively insensitive to the modification—increasing by about 12%. The interaction coefficient however increases by a factor of 3. Similar results may be expected for the predictions of this potential in other cases. Specifically, kink energies (for type A configurations) may increase by the same percentage as the step energy.

The step energies $\beta^0_{[\bar{1}\,\bar{1}2]}$ and $\beta^0_{[\bar{2}11]}$ computed here are comparable to the tight-binding calculation by Chadi and Chelikowsky[21] for configurations of type A. Their results, obtained using an energy minimization approach, are $\beta^0_{[\bar{1}\,\bar{1}2]} \approx 100$ meV/Å and $\beta^0_{[\bar{2}11]} \approx 182$ meV/Å. The SW results are in better agreement with these values. Surface energies computed by Chadi[22] (and the same predicted here from the step energies in the corresponding configurations) in eV/(1×1 unit cell area) are the following: (211) type A=1.4 (SW=1.24, KD=1.38); (211) type B=1.2 (SW=1.02), (311) type B=1.66 (SW=1.31) and (331) type A=1.09 (SW=1.29, KD=1.35). The (311) and (331) surface energies have been obtained by an extrapolation of the results obtained in this study to a terrace width (n_2) not studied. The surfaces composed of type B steps are comparable only to the results of SW potential since Chadi's calculations show that the rebonding occurs (similar to the SW potential) whereas this is not the case with the results of the KD potential.

Reconstructions observed using the SW potential agree qualitatively with those obtained by Wilson, Todd, Sutton[23] who used the same potential. They observed no reconstruction on the (110) surface, symmetric dimers on the (100) surface, and rebonded atoms on the (311) surface. Their values for the corresponding surface energies agree (to within 5%) to the same computed in this study: $[\epsilon_s(110)]_{SW}$=108.3 meV/Å^2, $[\epsilon_s(100)]_{SW}$=89.91 meV/Å^2, $[\epsilon_s(311)]_{SW}$=102.9 meV/Å^2 (the 311 surface requires an extrapolation of the results to a terrace width not studied). $[\epsilon_s(100)]_{SW}$ predicted here agrees with the same calculated by Poon *et al.*[12] Surface energy ratios calculated by Gilmer and Bakker[24] using the SW potential agree with those predicted here ($[\epsilon_s(110)/\epsilon_s(111)]_{SW}$ = 1.225, $[\epsilon_s(100)/\epsilon_s(111)]_{SW}$ = 1.059). The corresponding ratios for the KD potential are 1.246 and 1.234, respectively. They also find that reconstruction at the step edge reduces the $[\bar{1}\,\bar{1}2]$ step energy by an order of magnitude in relation to the bulk terminated step. This

TABLE IV. Energetics of kinked step configurations: (unkinked) step energy (β^0) and kink energy ϵ_k. n_1 and n_2 are the system dimensions, in units of the appropriate surface lattice constant, along the x and y axes, respectively. n_3 is the depth of the system in number of (111) bilayers.

		Kinked step configurations									
		SW potential					KD potential				
Configuration	Type	System size			Energetics		System size			Energetics	
		n_1 odd values	n_2	n_3	ϵ_k (meV)	β^0 (meV/Å)	n_1 odd values	n_2	n_3	ϵ_k (meV)	β^0 (meV/Å)
(IV) $\bar{1}\,\bar{1}2$ kink	A_1	5 to 13	7	9	220	162.0	3 to 11	11	9	798	240.2
		even values					even values				
$\Rightarrow 30° \geq \theta > 0°$	A_2	2 to 14	7	9	407	162.1	2 to 12	11	9	324	240.2
	B	1 to 7	21	9	785	40.4					
(V) $\bar{2}11$ kink	A	1 to 8	4	9	$\rightarrow -20^-$	previous value used	1 to 8	11	9	987	202.4
$\Rightarrow 30° \leq \theta < 60°$	B	1 to 8	11	9	$\rightarrow -1^+$	previous value used					

is the case here also for the configuration type B — the reduction being a factor of 9.7. From experiments on equilibrium shape of voids on Si(111) Eaglesham *et al.*[8] (and Follstaedt[25]) predict surface free energy (f_s) ratios, $f_s(100)/f_s(111) = 1.10 \pm 5\%$ (1.09 ± 0.07) and $f_s(110)/f_s(111) = 1.16 \pm 5\%$ (1.07 ± 0.03).

Table IV shows the results of simulations with the kink configurations. The orientational dependence of the step energy is obtained by varying the kink-kink separation ℓ_x (n_1) with a fixed terrace width (n_2) for configurations 3(f) to 3(j) in Fig. 3. The value of n_2 is chosen so that the terrace width is large enough to make the step-step interactions negligible, i.e., the contribution to the step energy in the worst case is less than 0.5%. The step energies β are therefore assumed to be equal to isolated step energies β^0. Kink energies ϵ_k are extracted by fitting the isolated step energy per unit length along the x axis β_x^0 to Eq. (8). Step energies along $\xi = 0$ are also extracted from these fits for comparison to previous results. The range of n_1 quoted in the table is the region over which these fits have been done. Figure 5 is typical of the straight line fits attempted. Success of this fitting procedure in most cases shows that kink-kink interactions are indeed negligible (beyond ≈ 5 lattice spacings). Further, the agreement between the step energies extracted here and those calculated previously also shows that kink-kink and step-step interactions (at the chosen values of n_2) are negligible. However this procedure fails for the $[\bar{2}11]$ kink when using the SW potential. This may be due to the kink energies being very small and possibly negative (as calculated using Eq. (8) with $\beta^0(\xi = 0)$ from previous calculations]. It may also be due to larger range of kink-kink interactions when using the SW potential.

The orientational dependence of the step energy β^0 vs θ is shown in the polar plots of Fig. 6. Plot 6(a) shows that the SW potential favors configurations of type B at least for $0 \leq \theta \leq 38°$. It is expected from plot 6(b) that the KD potential favors configurations of type B at least for $0 \leq \theta < 30°$. In both cases the lower energy configurations show a significant anisotropy in the step energy: for the SW case; $\beta^0_{[\bar{2}11]}/\beta^0_{[\bar{1}\bar{1}2]} \approx 4.8$ with $\beta^0_{[\bar{2}11]} - \beta^0_{[\bar{1}\bar{1}2]} \approx 150$ meV/Å and for the KD case; $\beta^0_{[\bar{1}01]}/\beta^0_{[\bar{2}11]} \approx 1.6$ with $\beta^0_{[\bar{1}01]} - \beta^0_{[\bar{2}11]} \approx 120$ meV/Å.

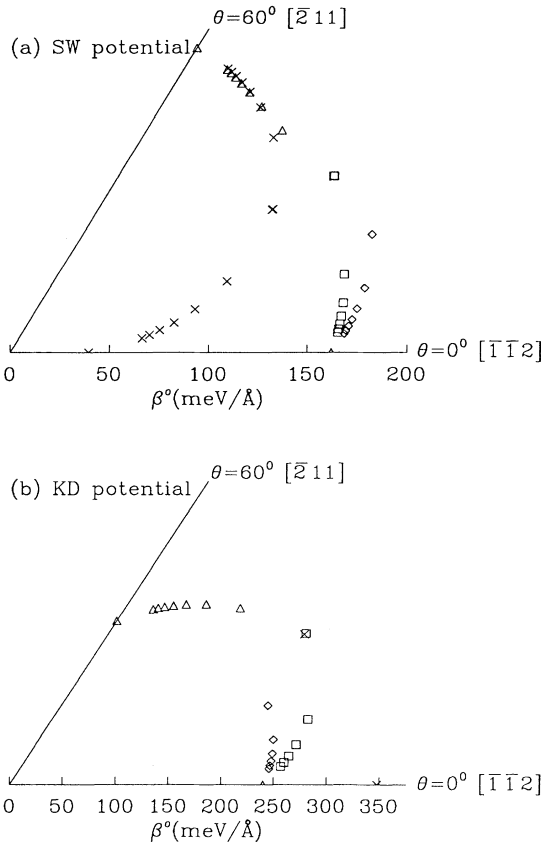

FIG. 6. Polar plots showing the variation of the step energy β^0 with orientation θ. □, ◇, △, and × correspond to configuration types A_1, A_2, A, and B, respectively. Lowest-energy configurations corresponding to both potentials show significant anisotropy in step energy inconsistent with experimental observations at high temperature.

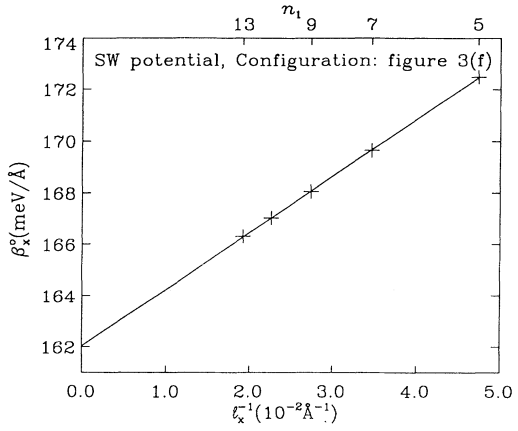

FIG. 5. Typical variation of the projected step energy β_x^0 with the kink-kink separation ℓ_x in a kink configuration. The linear variation of β_x^0 with ℓ_x^{-1} shows that the kink-kink interaction is negligible. The intercept is the step energy $\beta^0(\xi = 0)$ and the slope is the kink energy ϵ_k. The kink-kink separation is linearly related to n_1

IV. DISCUSSION

The empirical potentials used in this study have both been tuned to bulk properties of silicon. There has been no additional tuning to surface properties. Hence the energetics predicted here are only estimates of the quantitative values, but are expected to yield useful information about energetic trends. The robust results, i.e., common features predicted by both potentials are the following: (1) Step-step interactions vary as (terrace width)$^{-2}$ in particular range(s) of terrace width(s) consistent with elasticity theory; (2) negligible kink-kink interactions beyond ≈5 lattice spacings (in most cases); (3) in all cases

of nonzero step-step interaction, the interaction coefficient cannot be accounted for by the magnitude of the surface stress alone (see Appendix A)— the SW results in zero surface stress and the surface stress of the KD potential can account for an interaction coefficient of only ≈ 80 meV Å—hence the moment of in-plane forces must also exist in such cases (see Appendix A); (4) lowest-energy configurations calculated for both potentials show significant anisotropy in step energy in relation to the experimental temperature[1] of 101 meV. A rough estimate of anisotropy would be the maximal energy difference per unit length between steps of all possible orientations. Choosing the unit of length to be the lattice constant along the steps in the high symmetry directions, i.e., a_1 (=3.84 Å) this value is 574 meV (466 meV) for the lower energy configurations of the SW (KD) potential.

Using isotropic elastic theory (Appendix A) it can be seen that step-step interactions arise due to moments of the in-plane and normal forces that a step exerts on the underlying substrate. The very large step-step interactions predicted by the SW potential in configurations of type B, cannot however be due to the moment of the normal forces caused by the surface stress since it is predicted to be zero by this potential. Therefore, it is inferred that such a rebonding results in a large in-plane dipole moment (p_y). For the $[\bar{1}\,\bar{1}2]$ step of configuration type B, since the displacement of atoms on the terrace is towards the closer step edge, this moment has to be positive. Its value, for this step, using the computed value of the interaction coefficient, is 62 meV/Å. Interestingly, for steps on 7×7 reconstructed Si(111), from the experimental value of surface stress and the asymptotic displacement field of a step, p_z and p_y have been estimated[26] to be 0.58 ± 0.04 eV/Å and 1.46 ± 0.3 eV/Å.

Kink energies computed in this study show that they are not (in most cases) of a simple geometric origin, i.e., they cannot be derived from the energies of steps along the high symmetry directions. Since a kink of depth m units along a particular high symmetry direction (say, 1) is part of a step along the other high symmetry direction (say, 2), its energy in a simple geometric model (ϵ_k^G) would be

$$\epsilon_k^G(m) = (\beta_2^0 - \beta_1^0/2)ma_1, \tag{9}$$

where β_1^0 and β_2^0 are the step energies along the high symmetry directions 1 and 2, respectively, and a_1 is the lattice constant along either of the steps. Table V shows the derived and computed unit depth kink energies. Differences between them show that corner energies due to the presence and/or absence of rebonding at the kink site are significant and in some cases negative. The geometric model must therefore be extended to include a corner energy (e_c):

$$\epsilon_k(m) = (\beta_2^0 - \beta_1^0/2)ma_1 + e_c. \tag{10}$$

Two results in this study are apparently inconsistent with experimental observations. The first of these is the step-step interaction coefficient predicted by the SW potential for the configurations of type B. From the data of Alfonso *et al.*[1] on step distributions Williams *et al.*[7] determined the step-step interaction coefficient for the 1×1 phase of Si(111) to be 0.15 eV Å. The experimental estimate agrees roughly with the predictions of the KD potential but is about an order of magnitude smaller than the interaction coefficients predicted by the SW potential for configurations of type B. The rebonding between upper and lower terrace atoms predicted by the SW potential in such configurations results in large step-step interactions. Previous calculations[12] (using the SW potential) on the SB type step on Si(100) which has very similar rebonding along the step edge, i.e., between an atom with only two nearest neighbors and another with three in the bulk terminated configuration, have also shown that such a rebonding results in very large step-step interactions. For this step the interaction coefficient was computed to be 2.40±0.06 eV Å. Disagreement between the experimental estimate and the computed value of the interaction coefficient in this study therefore suggests that this rebonding does not occur for Si(111) steps, i.e., it is an "unphysical result."

However it must be noted that the same rebonding is predicted in the tight-binding calculations of Wilson, Todd, and Sutton[23] for the Si(311) surface and Chadi's[22] calculations for the Si(311) and Si(211) surfaces. The large interaction coefficient predicted here for $[\bar{1}\,\bar{1}2]$ steps is further supported by one of Ranke's[27] models for the Si(311) surface. The model explains the observed 3×2 periodicity on this surface by building it with $[\bar{1}\,\bar{1}2]$ steps with the configuration type being a "mixture" of types A and B, i.e., with some rebonding along the step edge (type A) and some between upper and lower terrace atoms (type B). Extrapolating the SW results it can

TABLE V. Comparison between kink energies derived from a simple geometric model (ϵ_k^G) [using Eq. (9) with $m = 1$] and the same computed directly in the simulations (ϵ_k). The corner energy $e_c = \epsilon_k - \epsilon_k^G$, is significant and in some cases negative.

		Geometric model for kink energies			
		SW potential		KD potential	
Configuration	Type	ϵ_k^G (meV)	ϵ_k (meV)	ϵ_k^G (meV)	ϵ_k (meV)
			220 (Type A_1)		798 (Type A_1)
(IV) $\bar{1}\,\bar{1}2$ kink	A	411	407 (Type A_2)	316	324 (Type A_2)
$\Rightarrow 30° \geq \theta > 0°$	B	648	785	109	
(V) $\bar{2}11$ kink	A	262	−20	533	987
$\Rightarrow 30° \leq \theta < 60°$	B	−211	−1	946	

be seen that the energy of this surface when built of steps of type B (=1.31 eV/1×1 unit cell area) is greater (but nearly degenerate) than if built with steps of type A (=1.26 eV/1×1 unit cell area). Hence, a mixture of configuration types (as modeled) may be lower in energy. In the rebonded configurations, as the rebonding is maximal for $[\bar{1}\,\bar{1}2]$ steps and not possible for $[\bar{2}11]$ steps it can be inferred from this study that the step-step interaction coefficient shows a strong orientational dependence with its magnitude in the range 0.0–4.5 eV Å. As the experimental estimate of the interaction coefficient has been derived for steps of unspecified orientation,[1] a study of the orientational dependence of the step-step interaction coefficient will resolve the problem of the presence or absence of rebonding unambiguously.[28]

The second apparent inconsistency with experiment is the large values of kink energy (and consequent large anisotropy in step energies) corresponding to the lower energy configurations of both potentials. From Alfonso's[1] estimate of step stiffness, Williams *et al.*[7] derive a kink energy of 0.23 eV in a square lattice Ising model. This gives the step energy in the square lattice model of 0.23 eV/a_1. A crude estimate of the anisotropy in a square lattice model with this step energy would be 95 meV which is smaller than the experimental temperature of 101 meV —disagreeing with similar estimates for the lowest energy configurations of the SW (574 meV) and KD (466 meV) potentials. This study suggests that anisotropy is unavoidable since if configurations of type B are lower in energy, then the rebonding (in such configurations where only one of the rebonding atoms is able to move, i.e., has two nearest neighbors when the system is bulk terminated whereas the other atom has three) would drastically reduce the energy of the $[\bar{1}\,\bar{1}2]$ step — as is the case with the SW potential. If configurations of type A are lower in energy then this rebonding would not occur and similar rebonding not occurring for the $[\bar{1}01]$ step would result in its step energy (in either configuration A or B) being high — as is the case with the KD potential.

Since the experimentally derived kink energy uses a square lattice model a Monte Carlo simulation was carried out on a hexagonal lattice for a step with an average orientation along the high symmetry direction(s). The aim of the simulation was to check if the hexagonal lattice allowed for a larger kink energy. The energy of the step is defined by a simple kink Hamiltonian of the form

$$H = H_0 + \sum_{i=0}^{N-1} \epsilon_k \mid y_i - y_{i+1} \mid , \qquad (11)$$

where $x_i = i \times a_\parallel$ with $a_\parallel = a_1/2$ and $y_i \times a_\perp = y(x_i)$ is an integral multiple of $a_\perp = a_2/2$. H_0 is the energy of a straight step, i.e., $H(\{y_i = 0\})$. It is a constant independent of the configuration $\{y_i\}$ and is therefore irrelevant for the simulation. Periodic boundary conditions are applied identifying x_0 and x_N where the system size N is chosen to be 800. The step positions y_i are moved according to the standard Metropolis algorithm at a temperature of k_bT. However the assumption of a single-valued y_i forces the following constraints on a hexagonal lattice: (1) Neighboring step positions can differ maximally by only one unit equal to $a_\perp$, (2) a particular step position cannot be changed without a correlated change in at least one of the neighboring step positions, and (3) since correlated changes of only nearest neighbor step positions are allowed, some step positions cannot be changed in particular configurations of their nearest neighbors. The simulation is run beginning from a straight step until equilibrium is reached. This is detected through the saturation of the squared width (see Appendix B). Defining the Monte Carlo unit of time to be N attempts to change randomly chosen step positions, equilibrium is reached for the system size of $N = 800$ around 8×10^3 time units at the largest value of the ratio ϵ_k/k_bT considered in this study. The simulation is run until twice this time for all values of this ratio thus ensuring that averages computed beyond $t = 8\times10^3$ time units correspond to equilibrium averages. The spatial correlation function $G(x,t)$ (see Appendix B) is computed as an average over 50 such runs. Further, time averaging, using 21 equally time-spaced values of $G(x,t)$ between $t = 12 \times 10^3$ and $t = 16 \times 10^3$, is assumed to give the equilibrium spatial correlation function $G_{\rm eq}(x)$.

The assumption of a single valued y_i may have eliminated configurations of significant weight in the partition function corresponding to a more general Hamiltonian which allows for multi-valued y_i. However, the typical equilibrium step configuration, with ϵ_k/k_bT corresponding to the smallest nonzero value of kink energy (220 meV) and the experimental temperature[1] of 101 meV, shows only unit depth kinks or antikinks [Fig. 7(a)]. It can therefore be argued that the constraints imposed by the assumption of a single-valued y_i eliminate only con-

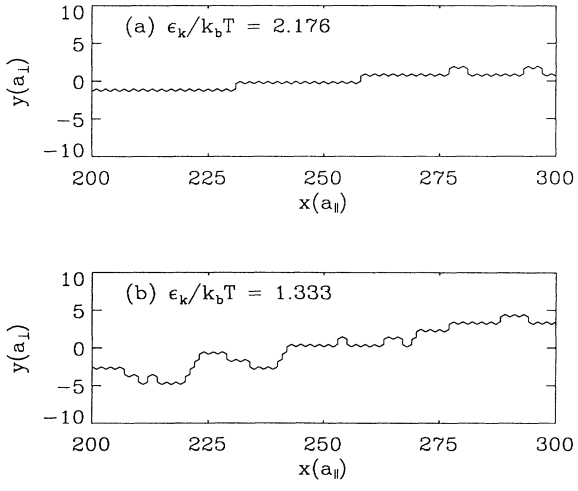

FIG. 7. Typical equilibrium step configurations from Monte Carlo simulation: the configuration with larger kink energy has only unit depth kinks-antikinks whereas the configuration with smaller kink energy has kinks-antikinks of more than unit depth. Hence, the step stiffness (shown in Fig. 8), computed from the spatial correlation function, is expected to be unaffected by the assumption of a single-valued $y(x)$, at and above the larger value of kink energy. $a_\parallel$ and $a_\perp$ are half of the surface lattice constants a_1 and a_2, respectively.

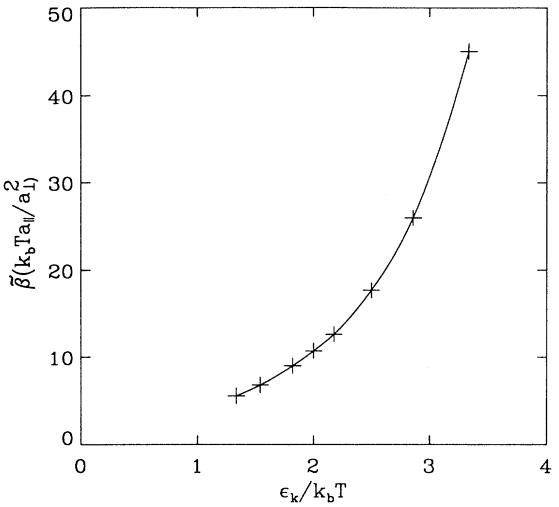

FIG. 8. Variation of the step stiffness $\tilde{\beta}$ with the ratio of the kink energy (ϵ_k) and the temperature (k_bT). Only the unfavorable configuration to the SW potential (type A_1) gives a small enough kink energy whose corresponding stiffness is roughly consistent with experimental observations. $a_{\|}$ and $a_{\perp}$ are half of the surface lattice constants a_1 and a_2, respectively.

figurations of negligible weight. The results of this simulation are therefore assumed to be correct at and beyond this value of kink energy. At smaller values of ϵ_k/k_bT the results may be in error: Fig. 7(b) shows the typical equilibrium step configuration at the smallest value of ϵ_k/k_bT considered in this study. Since there are kinks-antikinks of more than unit depth, configurations of significant weight may have been eliminated.

The step stiffness $\tilde{\beta}$ is extracted from the linear relationship between $G_{eq}(x)$ and x for "small" (here $x \leq 10a_{\|}$) values of x (see Appendix B). Figure 8 shows the variation of $\tilde{\beta}$ with ϵ_k/k_bT. Using the experimental temperature of 101 meV the figure gives a stiffness of 0.22 eV/Å when ϵ_k=220 meV. Since the experimental value of stiffness is smaller (0.14 eV/Å) and since the corresponding kink energy derived in a square lattice model is 230 meV it can be concluded that the hexagonal lattice is stiffer than a square lattice at least around this value of ϵ_k/k_bT, i.e., does not permit larger kink energies. Further, since the step stiffness increases rapidly with ϵ_k/k_bT (as shown in Fig. 8), its value is much larger than the experimental value for the kink energies corresponding to the lowest energy configurations of both the SW and KD potentials (and a temperature of 101 meV). Hence, the hexagonal lattice does not resolve the inconsistency between experiment and the results of this study.

V. CONCLUSION

Energetics of vicinal Si(111) steps with 1×1 terraces, calculated using the empirical potentials of Stillinger-Weber and Khor–Das Sarma, show that rebonding between upper and lower terrace atoms results in step-step interactions much larger than experimental estimates. This suggests that such a rebonding does not occur. These calculations also show that the variation of step energy with terrace width is consistent with elasticity theory with the step-step interactions being not only due to surface stress but also due to in-plane force moments at the step edges. Calculations on the orientational dependence of the step energy show that kink-kink interactions are negligible beyond ≈ 5 lattice spacings and that there are significant corner energies. Differences between the predictions of the two potentials can be interpreted as being due to their differing with regard to bond bending: the SW potential is very "soft" and therefore allows two atoms to rebond even if only one of the rebonding atoms is able to move (i.e., has before rebonding only two nearest neighbors while the other has three) whereas the KD potential is very "hard," allowing rebonding only if both atoms can move. Two unresolved problems are brought out in this study: (a) configurations with rebonding between upper and lower terrace atoms although inconsistent with experiments probing step-step interactions are however the lowest energy configurations. This rebonding is further supported by a model for the Si(311) surface and other tight-binding calculations for the Si(211) and Si(311) surfaces and (b) the kink energies corresponding to the lowest energy configurations of both potentials give a step stiffness much higher than the experimental value. Possible resolutions to these problems may lie in tuning the empirical potential to surface-step properties. Also since adatom coverage is significant[29] around the temperature of 900°C (20–22% of a monolayer), zero-temperature energetics of configurations with adatoms may be more appropriate for use in statistical mechanical models explaining the experimental observations on step fluctuations and step-step interactions.

ACKNOWLEDGMENTS

One of the authors (S. Kodiyalam) wishes to thank Dr. T.L. Einstein, S.V. Khare, P.I. Tamborenea, and C.J. Lanczyki for useful discussions. This work was supported by the NSF-MRG and the U.S. ONR.

APPENDIX A: ELASTICITY THEORY OF STEP-STEP INTERACTIONS

In this section elasticity theory has been used to estimate the step-step interaction coefficient. A step is assumed to create a force distribution on the surface. The distribution causes displacements in the substrate. Steps therefore interact through the interference of their respective displacement fields.

Assuming that the step is along the x direction (at $y = 0$), invariance along the step implies that there is no x component to these forces and that the distribution is independent of x. Further, assuming that the surface is at constant z, the force distribution $\vec{F}(y) = F_y(y)\hat{j} +$

$F_z(y)\hat{k}$ may be approximated by the zeroth (monopole) and the first (dipole) moments of the $F_y(y)$ and $F_z(y)$ about the step edge $y = 0$. From the work of Stewart, Pohland, and Gibson,[26] on a surface with an isotropic stress tensor [as is the case with Si(111)] the distribution created by a step has vanishing monopole moments and the dipole moment corresponding to $F_z(y)$ must be equal in magnitude to the product of the surface stress σ and the step height h. Hence, $\vec{F}(y)$ is approximated by

$$\vec{F}(y) = p_y\delta(y)\hat{j} + p_z\delta(y)\hat{k} \ , \tag{A1}$$

where p_y is the dipole moment of the in-plane forces F_y, and p_z is the dipole moment of the forces perpendicular to the plane F_z which is given by

$$p_z = +\sigma h, \tag{A2}$$

with the positive y axis in the step down direction.

From the work of Rickman and Srolovitz,[18] for an elastically isotropic medium the interaction energy for two force distributions of the above form separated by a distance ℓ along the y axis varies as $\bar{A}/\ell^2$, with $\bar{A}=2(1-\nu^2)(p_y^2+p_z^2)/(\pi E)$ where E is the Young's modulus and ν is the Poisson's ratio for the medium [the displacement field in the y direction due to the single force distribution at $y = 0$ is given by $-2(1-\nu^2)p_y/(\pi E y)$]. Due to the $1/\ell^2$ variation of the interaction energy a periodic array of steps will have an interaction coefficient A greater than $\bar{A}$ by a factor of $\pi^2/6$, i.e.,

$$A = \pi(1-\nu^2)(p_y^2+p_z^2)/(3E). \tag{A3}$$

Assuming silicon to be elastically isotropic, the above expression is used in the text to calculate the contribution of the surface stress to the step-step interaction coefficient and also the dipole moment p_y given A and p_z. The Poisson's ratio $\nu = c_{12}/(c_{11}+c_{12})$ and the Young's modulus $E = (c_{11}-c_{12})(1+\nu)$ where c_{11} and c_{12} are elastic constants of silicon computed by Ito, Khor, and Das Sarma.[30]

APPENDIX B: EQUILIBRIUM STATISTICAL MECHANICS OF STEP FLUCTUATIONS

In this section equilibrium statistical mechanics has been used to derive the functional form of the spatial correlation function $G_{\rm eq}(r)$. The fluctuations of a step along the x axis are described by a coarse-grained free energy functional,[31] or effective Hamiltonian, for configurations $y(x)$.

In the absence of any potential and neglecting terms independent of the configuration the effective Hamiltonian can be written as

$$H = \int_0^L \tilde{\beta}\left(\frac{\partial y}{\partial x}\right)^2 dx \ , \tag{B1}$$

where $\tilde{\beta}$ is the step stiffness and L is the length over which periodic boundary conditions are applied. The equilibrium squared width W may now be evaluated by calculating the expectation value of $[y(x)]^2$ and $y(x)$ in the canonical ensemble. Due to translational invariance these quantities are independent of x and therefore can be averaged over x. Hence,

$$W_{\rm eq} = \langle\langle\, [y(x)]^2 \ - \ \langle y(x)\rangle_x^2 \,\rangle_x\rangle \ . \tag{B2}$$

Similarly, the equilibrium spatial correlation function $G_{\rm eq}(x, x+r)$ may now be evaluated by calculating the expectation value of $[y(x)-y(x+r)]^2$. Hence,

$$G_{\rm eq}(r) = \langle\langle\, [y(x)-y(x+r)]^2\rangle_x\rangle \tag{B3}$$

with the Hamiltonian as specified before.

Calculating the above using Fourier components of $y(x)$ gives

$$G_{\rm eq}(r) = \frac{k_bT}{\tilde{\beta}} r\left(1-\frac{r}{L}\right) \ . \tag{B4}$$

Hence, in a Monte Carlo simulation, the linear relationship between $G(r)$ and r for small r ($\frac{r}{L} \ll 1$) can be used to determine $\tilde{\beta}$.

[1] C. Alfonso, J.M. Bermond, J.C. Heyraud, and J.J. Metois, Surf. Sci. **262**, 371 (1992).
[2] N.C. Bartelt, J.L. Goldberg, T.L. Einstein, and E.D. Williams, Phys. Rev. B **48**, 15 453 (1993).
[3] L. Kuipers, M.S. Hoogeman, and J.W.M. Frenken, Phys. Rev. Lett. **71**, 3517 (1993).
[4] M. Giesen-Seibert, R. Jentjens, M. Poengsen, and H. Ibach, Phys. Rev. Lett. **71**, 3521 (1993).
[5] M. Poengsen, J.F. Wolf, J. Frohn, M. Giesen, and H. Ibach, Surf. Sci. **274**, 430 (1992).
[6] N.C. Bartelt, J.L. Goldberg, T.L. Einstein, and E.D. Williams, Surf. Sci. **273**, 252 (1992).
[7] E.D. Williams, R.J. Phaneuf, Jian Wei, N.C. Bartelt, and T.L. Einstein, Surf. Sci. **294**, 219 (1993).
[8] D.J. Eaglesham, A.E. White, L.C. Fieldman, N. Moriya, and D.C. Jacobson, Phys. Rev. Lett. **70**, 1643 (1993).
[9] R.M. Tromp (private communication).
[10] F.H. Stillinger and T.A. Weber, Phys. Rev. B **31**, 5262 (1985).
[11] K.E. Khor and S. Das Sarma, Phys. Rev. B **36**, 7733 (1987).
[12] T.W. Poon, S. Yip, P.S. Ho, and F.F. Abraham, Phys. Rev. Lett. **65**, 2161 (1990).
[13] O.L. Alerhand, David Vanderbilt, Robert D. Meade, and J.D. Joannopoulos, Phys. Rev. Lett. **61**, 1973 (1988).
[14] X.P. Li, P.B. Allen, and J.Q. Broughton, Phys. Rev. B **38**, 3331 (1988).
[15] K.E. Khor and S. Das Sarma, Phys. Rev. B **38**, 3318 (1988).
[16] K.E. Khor and S. Das Sarma, Phys. Rev. B **39**, 1188 (1989).
[17] C.W. Gear, *Numerical Initial Value Problems in Ordinary*

Differential Equations (Prentice-Hall, Englewood Cliffs, N.J., 1971).
[18] J.M. Rickman and D.J. Srolovitz, Surf. Sci. **211**, 211 (1993).
[19] R. Shuttleworth, Proc. Phys. Soc. London Sect. A **63**, 444 (1950).
[20] David Vanderbilt, Phys. Rev. Lett. **59**, 1457 (1987).
[21] D.J. Chadi and J.R. Chelikowsky, Phys. Rev. B **24**, 4892 (1981).
[22] D.J. Chadi, Phys. Rev. B **29**, 785 (1984).
[23] J.H. Wilson, J.D. Todd, and A.P. Sutton, J. Phys. Condens. Matter **2**, 10 259 (1991).
[24] G.H. Gilmer and A.F. Bakker, in *Defects in Materials*, edited by P.D. Bristowe, J.E. Epperson, J.E. Griffith, and Z. Liliental-Weber, MRS Symposia Proceedings No. 209 (MRS, Pittsburgh, l991), p. 135.
[25] D.M. Follstaedt, Appl. Phys. Lett. **62**, 1116 (1993).
[26] J. Stewart, O. Pohland, and J.M. Gibson, Phys. Rev. B **49**, 13 848 (1994).
[27] W. Ranke, Phys. Rev. B **41**, 5243 (1990).
[28] Dr. J.J. Metois (private communication). However, this suggests that there is no orientational dependence in the interaction coefficient.
[29] Y.N. Yang and E.D. Williams, Phys. Rev. Lett. **72**, 1862 (1994).
[30] T. Ito, K.E. Khor, and S. Das Sarma, Phys. Rev. B **40**, 9715 (1989).
[31] N.C. Bartelt, T.L. Einstein, and E.D. Williams, Surf. Sci. Lett. **240**, L591 (1990), and references therein